Autophagy 11:12, 2172–2183; December 2015; © 2015 Taylor & Francis Group, LLC

A new microRNA signal pathway regulated by long noncoding RNA TGFB2-OT1 in autophagy and inflammation of vascular endothelial cells

ShuYa Huang,[1] Wei Lu,[1] Di Ge,[1] Ning Meng,[2] Ying Li,[1] Le Su,[1] ShangLi Zhang,[1] Yun Zhang,[3] BaoXiang Zhao,[2] and JunYing Miao[1,3,*]

[1]Shandong Provincial Key Laboratory of Animal Cells and Developmental Biology; School of Life Science; Shandong University; Jinan, China; [2]Institute of Organic Chemistry; School of Chemistry and Chemical Engineering; Shandong University; Jinan, China; [3]The Key Laboratory of Cardiovascular Remodeling and Function Research; Chinese Ministry of Education and Chinese Ministry of Health; Qilu Hospital; Shandong University; Jinan, China

Keywords: 3′UTR-derived RNA, autophagy, ceRNA, inflammation, lncRNA, microRNA

Abbreviations: 3BDO, 3-benzyl-5-((2-nitrophenoxy) methyl)-dihydrofuran-2(3H)-one; 3′UTR, 3′ untranslated region; ATG13, autophagy-related 13; CeRNA, competing endogenous RNA; CERS1, ceramide synthase 1; HUVECs, human umbilical vein endothelial cells; IL6, interleukin 6; IL8, interleukin 8; IL1B, interleukin 1, β; LARP1, La ribonucleoprotein domain family, member 1; lncRNA, long noncoding RNAs; LPS, lipopolysaccharide; *MIR3960*, microRNA 3960; *MIR4459*, microRNA 4459; *MIR4488*, microRNA 4488; miRNA, microRNA; NAT8L, N-acetyltransferase 8-like (GCN5-related, putative); NUPR1, nuclear protein, transcriptional regulator, 1; oxLDL, oxidized low-density lipoprotein; qPCR, quantitative real-time PCR; SQSTM1, sequestosome 1; TGFB2, transforming growth factor, β 2; *TGFB2-OT1*, TGFB2 overlapping transcript 1; TIA1, TIA1 cytotoxic granule-associated RNA binding protein; VECs, vascular endothelial cells.

TGFB2-OT1 (*TGFB2* overlapping transcript 1) is a newly discovered long noncoding RNA (lncRNA) derived from the 3′UTR of TGFB2. It can regulate autophagy in vascular endothelial cells (VECs). However, the mechanisms of *TGFB2-OT1* action are unclear, and whether it is involved in VECs dysfunction needs investigation. Here, the level of *TGFB2-OT1* was markedly increased by lipopolysaccharide and oxidized low-density lipoprotein, 2 VECs inflammation triggers. A chemical small molecule, 3-benzyl-5-((2-nitrophenoxy) methyl)-dihydrofuran-2(3H)-one (3BDO) significantly decreased *TGFB2-OT1* levels and inhibited the effect of LPS and oxLDL. The NUPR1 level was upregulated by the 2 inflammation inducers and modulated the *TGFB2-OT1* level by promoting the expression of TIA1, responsible for *TGFB2-OT1* processing. We focused on how *TGFB2-OT1* regulated autophagy and inflammation. Use of miRNA chip assay, *TGFB2-OT1* overexpression technology and 3BDO revealed that *TGFB2-OT1* regulated the levels of 3 microRNAs, *MIR3960, MIR4488* and *MIR4459*. Further studies confirmed that *TGFB2-OT1* acted as a competing endogenous RNA, bound to *MIR3960, MIR4488* and *MIR4459*, then regulated the expression of the miRNA targets CERS1 (ceramide synthase 1), NAT8L (N-acetyltransferase 8-like [GCN5-related, putative]), and LARP1 (La ribonucleoprotein domain family, member 1). CERS1 and NAT8L participate in autophagy by affecting mitochondrial function. *TGFB2-OT1* increased the LARP1 level, which promoted SQSTM1 (sequestosome 1) expression, NFKB RELA and CASP1 activation, and then production of IL6, IL8 and IL1B in VECs. Thus, NUPR1 and TIA1 may control the level of *TGFB2-OT1*, and *TGFB2-OT1* bound to *MIR3960, MIR4488* and *MIR4459*, which targeted CERS1, NAT8L, and LARP1, respectively, the key proteins involved in autophagy and inflammation.

Introduction

In recent years, numerous studies have documented that only 2% of the mammalian genome is composed of genes that encode proteins. This finding is particularly surprising because most human genes are transcribed as noncoding RNA.[1] Long noncoding RNAs (lncRNAs) are defined as nonprotein-coding transcripts longer than 200 nucleotides that represent a large portion of the mammalian transcriptome.[2] Whether these lncRNAs participate in important cellular functions or merely represent transcriptional noise remains a matter of debate in the initial phases of study.[3,4]

The roles of lncRNAs in regulating gene transcription have been extensively studied. Some lncRNAs interact with chromatin-modifying enzymes and regulate the transcriptional activation or silencing of some genes. For example, the lncRNA *XIST* participates in the inactivation of one X chromosome.[5-8] Some lncRNAs are involved in post-transcriptional gene regulation.

*Correspondence to: JunYing Miao; Email: miaojy@sdu.edu.cn; BaoXiang Zhao; Email: bxzhao@sdu.edu.cn
Submitted: 03/19/2015; Revised: 09/28/2015; Accepted: 10/06/2015
http://dx.doi.org/10.1080/15548627.2015.1106663

LncRNA *MALAT1* (metastasis-associated lung adenocarcinoma associated transcript 1) can sequester serine/arginine proteins to modulate pre-mRNA alternative splicing.[9]

MicroRNAs (miRNAs) are small, 19- to 22-nucleotide sequences of noncoding RNA that mostly work as gene expression regulators.[10] The crossregulation between lncRNAs and miRNAs has attracted increasing interest. This crossregulation can be artificially divided into 4 forms.[11] First, miRNAs target lncRNAs and reduce lncRNA stability. The miRNA *MIRLET7B* contributes to lowering *TP53COR1* stability in human cervical carcinoma cells.[12] Additionally, the recruitment of *MIRLET7* decreases the stability of another lncRNA, *HOTAIR*.[13] Second, lncRNAs compete with miRNAs to bind with the common target mRNAs. *BACE1-AS* is an antisense lncRNA of *BACE1* (β-site APP-cleaving enzyme 1). In HEK293 cells, *MIR485* overexpression reduces *BACE1* mRNA level, which is rescued by overexpressing *BACE1-AS*, complementary to *BACE1* mRNA in a region that contains the *MIR485* binding site.[14] Third, lncRNAs generate miRNAs to induce target mRNA silencing. *LINCMD1* can generate *MIR206* and *MIR133B* from an intron and an exon.[15] LncRNA *H19* can also generate *MIR675*.[16] Finally, lncRNAs act as molecular decoys or "sponges" of miRNAs. These lncRNAs are known as competing endogenous RNAs (ceRNAs).[17] CeRNAs share the same miRNA recognition sequences with mRNAs and compete for miRNA binding and then affect the regulation and functions of target mRNAs. CeRNA was first described by Poliseno and colleagues,[18] who report that the expression of the tumor suppressor *PTEN* (phosphatase and tensin homolog) depends on the expression of the pseudogene *PTENP1* transcript. *PTENP1* can act as a decoy for miRNAs targeting *PTEN* mRNA and affect *PTEN* expression. Despite the extensive existence and abundant expression of lncRNAs, their functions have been rarely revealed. Research into mammalian lncRNAs that sponge miRNAs from target binding mRNAs has focused on muscle differentiation and stem-cell self-renewal.

In a previous study, we have used the small chemical molecule 3-benzyl-5-((2- nitrophenoxy) methyl)-dihydrofuran-2(3H)-one (3BDO) and have identified a novel long noncoding RNA, *TGFB2-OT1* (TGFB2 overlapping transcript 1), located in the 3′UTR (3′ untranslated region) of *TGFB2* (transforming growth factor, β 2). *TGFB2-OT1* can sequester *MIR4459* (microRNA 4459), regulate the level of the *MIR4459* target ATG13 (autophagy related 13) and then promote autophagy.[19] Our subsequent study shows that 3BDO can inhibit the production of inflammatory cytokines both in vitro and in vivo.[20] Autophagy and inflammation are very closely related processes. Autophagy can be induced by the inflammatory response and modulate it.[21,22]

SQSTM1 (sequestosome 1) is a multifunctional scaffold protein that participates in various processes, including signal transduction, cell proliferation, cell survival and death, inflammation, tumorigenesis, and oxidative stress response. SQSTM1 is an autophagy substrate and widely used marker of autophagic degradation but also acts as a scaffold of numerous interacting proteins that promote the interaction of effector proteins with their substrates, and then transmits the signal downstream to activate NFKB signal pathway.[23] Previous studies show that SQSTM1 also activates CASP1 (caspase 1, apoptosis-related cysteine peptidase) and then increases IL1B (interleukin 1, β) levels.[24]

In this study we first observed that the inflammation inducers lipopolysaccharide (LPS) and oxidized low-density lipoprotein (oxLDL) elevated the level of *TGFB2-OT1*, and 3BDO inhibited this effect, then we investigated the underlying mechanisms of autophagy and inflammation induced by *TGFB2-OT1*, possibly via SQSTM1.

Results

LPS and oxLDL increased TGFB2-OT1 levels and 3BDO inhibited this process

To understand the relationship between *TGFB2-OT1* and vascular endothelial cells (VECs) inflammation, we first investigated the effects of LPS and oxLDL, inducers of human umbilical VECs (HUVECs) inflammation, on the level of *TGFB2-OT1*. LPS stimulation increased *TGFB2-OT1* RNA level in HUVECs, which was significantly inhibited by 3BDO (**Fig. 1A**). LPS increased *TGFB2-OT1* mRNA level dose- and time-dependently, which was also reversed by 3BDO (**Fig. 1B-C**). In addition, oxLDL increased *TGFB2-OT1* level, which was reversed by 3BDO.(**Fig. 1D**)

LPS and oxLDL elevated NUPR1 (nuclear protein, transcriptional regulator, 1) and TIA1 (TIA1 cytotoxic granule-associated RNA binding protein) levels

Our previous study shows that LPS induces the expression of the NUPR1,[25] and TIA1 is responsible for processing *TGFB2-OT1*.[19] However, the effect of oxLDL on NUPR1 and TIA1 levels and whether LPS affects TIA1 expression are unclear. Here, we showed that oxLDL increased NUPR1 levels, and 3BDO inhibited this effect (**Fig. 2A**). Similarly both oxLDL and LPS increased TIA1 protein levels, and 3BDO inhibited these effects. (**Fig. 2B**)

NUPR1 and TIA1 regulated TGFB2-OT1 level

Next, we determined the role of NUPR1 in regulating *TGFB2-OT1* level. When *NUPR1* was knocked down, LPS did not increase the level of *TGFB2-OT1* in HUVECs (**Fig. 3A-B**). In our previous study, we demonstrated that TIA1 is responsible for *TGFB2-OT1* processing, and knockdown of *TIA1* decreases the *TGFB2-OT1* level.[19] Here we further indicated that when *TIA1* was knocked down, LPS did not increase *TGFB2-OT1* levels (**Fig. 3C**). Furthermore, when *NUPR1* was knocked down, LPS did not increase the TIA1 level (**Fig. 3D**). NUPR1 may modulate the expression of TIA1 responsible for processing *TGFB2-OT1*.

TGFB2-OT1 regulated the levels of MIR3960 and MIR4488

In a previous study, we showed that *TGFB2-OT1* binds to *MIR4459*, modulates the expression of ATG13, an *MIR4459* target, and then participates in autophagy.[19] Moreover, our

bioinformatics analysis revealed that 57 presumed miRNAs could recognize and bind to *TGFB2-OT1* (http://bioinfo.uni-plovdiv.bg/microinspector/). So we further detected new miRNAs regulated by *TGFB2-OT1* in this study.

We first performed an miRNA microarray assay to identify miRNAs with changed expression when *TGFB2-OT1* was up- or downregulated (**Fig. S1**). We considered both bioinformatics analysis and microarray assay results and identified the top 5 miRNAs, including *MIR3960, MIR4459, MIR149-3p, MIR4688* and *MIR4488*, with significantly changed expression (**Table S2**). We excluded *MIR4688* because of low expression in HUVECs and *MIR149-3p* because we did not find an appropriate *MIR149-3p* target involved in autophagy or inflammation. We further chose *MIR3960* and *MIR4488*, which could bind to *TGFB2-OT1* and showed significantly changed expression on miRNA array assay. We verified the miRNA microarray results by qPCR. *TGFB2-OT1* downregulation by 3BDO increased and *TGFB2-OT1* overexpression decreased the levels of *MIR3960* and *MIR4488*. (**Fig. 4A-B**)

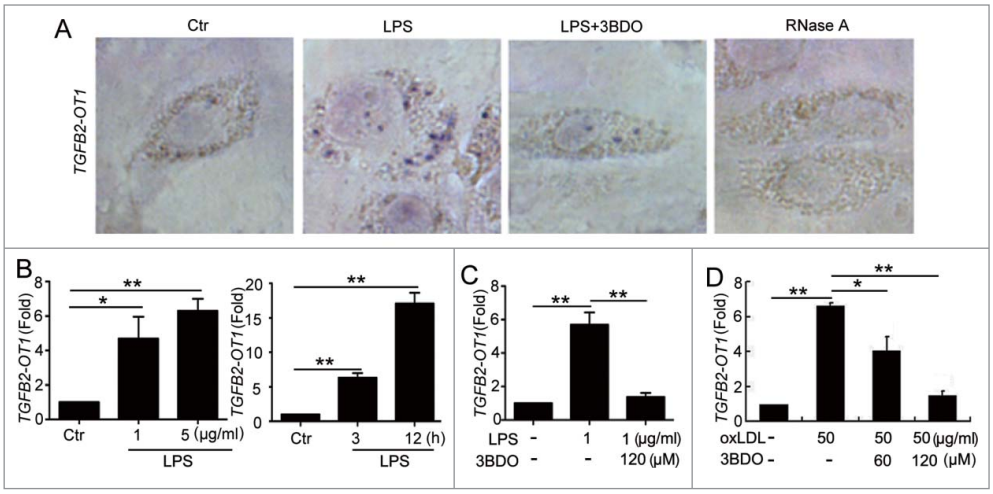

Figure 1. The increased *TGFB2-OT1* level induced by LPS and oxLDL was inhibited by 3BDO. (**A**) LPS increased *TGFB2-OT1* expression and 3BDO (120 μM) inhibited the increase of *TGFB2-OT1* induced by 1 μg/ml LPS for 12 h in HUVECs with in situ hybridization. (**B**) Quantified real-time PCR analysis of RNA levels of *TGFB2-OT1* after HUVECs were exposed to 1 μg/ml or 5 μg/ml LPS for 3 h, and treated with 1 μg/ml LPS for 3 h or 12 h. (**C**) Quantified real-time PCR analysis of *TGFB2-OT1* expression in HUVECs treated with 1 μg/ml LPS in presence or absence of 120 μM 3BDO for 3 h. (**D**) HUVECs were exposed to 50 μg/ml nLDL and oxLDL in presence or absence of 3BDO (60 μM and 120 μM) for 24 h, then *TGFB2-OT1* levels were determined by qPCR. *, $P < 0.05$; **, $P < 0.01$; n = 3.

MIR3960 and MIR4488 directly bind to TGFB2-OT1

According to the prediction results, *TGFB2-OT1* has one putative *MIR3960* binding site at positions 623 to 642 and one putative *MIR4488* binding site at positions 619 to 636. So we recombined the *TGFB2-OT1* cDNA (Luc-*TGFB2-OT1*-WT) and mutational cDNA with the presumed *MIR3960* and *MIR4488* deleted recognition sequences (Luc-*TGFB2-OT1*-3960Δ and Luc-*TGFB2-OT1*-4488Δ) downstream the luciferase reporter gene (**Fig. S2A and B**). The vectors were transfected in HEK293 cells along with the corresponding miRNA mimics. With *MIR3960* and *MIR4488* mimics transfection, luciferase activity was reduced by about 60% and 40% respectively, as compared with control miRNA. When adding mutant substrates for *MIR3960* and *MIR4488*, the decreased luciferase activity was abolished (**Fig. 4C-D**). Therefore, *MIR3960* and *MIR4488* directly bind *TGFB2-OT1*.

MIR3960, MIR4488 and *MIR4459* targeted the 3′UTRs of *CERS1* (ceramide synthase 1), *NAT8L* (N-acetyltransferase

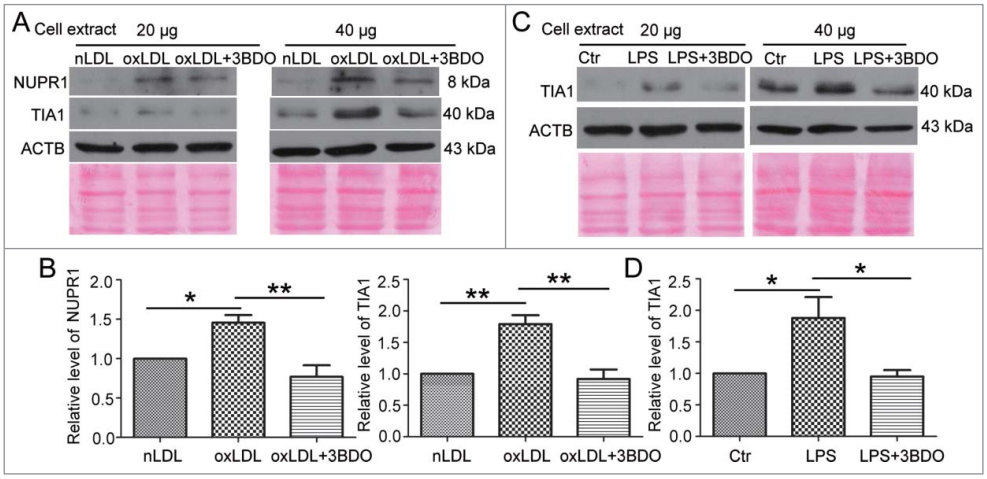

Figure 2. The increased NUPR1 and TIA1 levels induced by LPS and oxLDL were inhibited by 3BDO. (**A**) HUVECs were exposed to 50 μg/ml nLDL or oxLDL with or without 3BDO (60 μM) for 24 h, then 20 and 40 μg cell extracts was loaded on the SDS-PAGE respectively. Western blot analysis of NUPR1 and TIA1 protein levels, with ACTB and Ponceau staining as the loading control, and (**B**) quantification. (**C**) HUVECs were treated with LPS (1 μg/ml, 6 h) with or without 3BDO (60 μM), then 20 and 40 μg cell extracts was loaded on SDS-PAGE respectively. Western blot analysis of TIA1 protein level, with ACTB and Ponceau staining as the loading control, and (**D**) quantification. *, $P < 0.05$; **$P < 0.01$; n = 3.

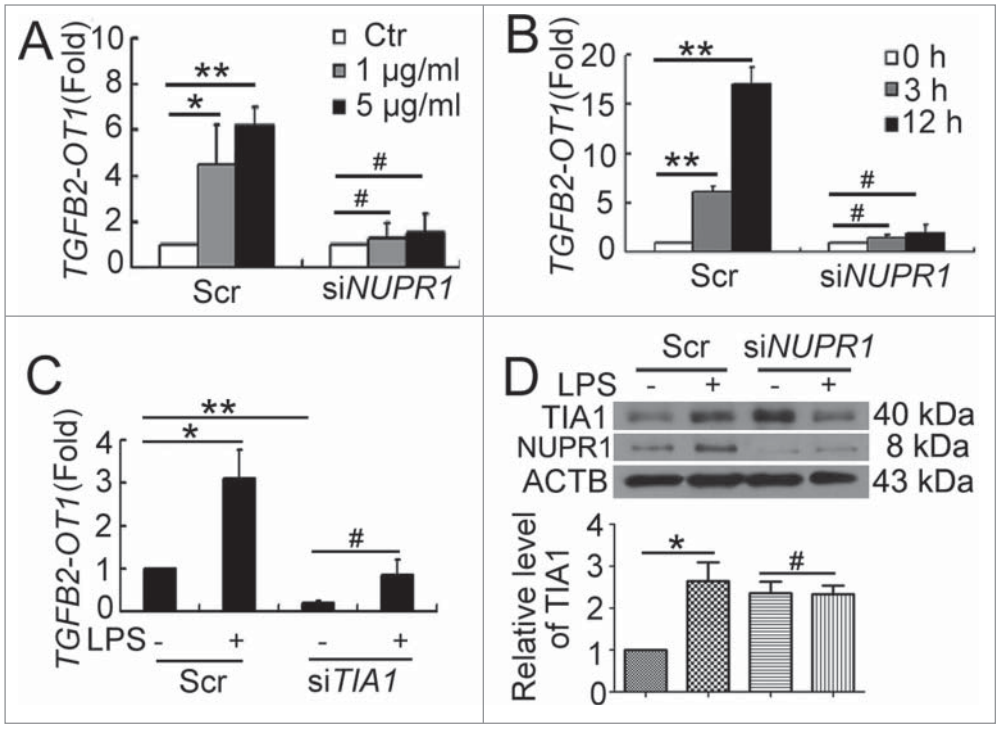

Figure 3. NUPR1 and TIA1 were involved in regulation of *TGFB2-OT1* level. qPCR analysis of *TGFB2-OT1* mRNA levels in HUVECs subjected to scrambled siRNA (Scr) or *NUPR1* siRNA (si*NUPR1*, 40 nM) for 24 h, then exposed to LPS at various concentrations for 3 h (**A**) or treated with 1 μg/ml LPS for 3 or 12 h (**B**). (**C**) qPCR analysis of *TGFB2-OT1* mRNA levels in HUVECs subjected to scrambled siRNA (Scr) or *TIA1* siRNA (si*TIA1*, 40 nM) for 24 h, then treated with 1 μg/ml LPS for 6 h. (**D**) Western blot analysis of the TIA1 protein level in HUVECs subjected to scrambled siRNA (Scr) or NUPR1 siRNA (si*NUPR1*, 40 nM) for 24 h, then exposed to 1 μg/ml LPS for 6 h. *, $P < 0.05$; **, $P < 0.01$; #, $P > 0.05$; n = 3.

8-like [GCN5-related, putative]) and *LARP1* (La ribonucleoprotein domain family, member 1), respectively.

Next, we predicted the downstream targets of *MIR3960* and *MIR4488* by bioinformatics analysis. We selected CERS1 as an *MIR3960* target protein and NAT8L as an *MIR4488* target protein, both involved in regulating autophagy by affecting mitochondria.[26,27] We first examined the modulation of miRNA on the targets. HUVECs were transfected with *MIR3960* and *MIR4488* mimics or inhibitor. The efficiency of miRNA mimics and inhibitor was determined by qPCR. miRNA mimics and the inhibitor at 25 and 50 nM effectively increased or decreased the corresponding miRNA level, respectively (**Fig. S3A**). We further determined the mRNA level of miRNA targets by transfecting HUVECs with miRNA mimics or inhibitor. miRNA mimics decreased the corresponding target mRNA levels, and miRNA inhibitor increased the corresponding target mRNA levels (**Fig. S3B**).

Furthermore, we determined the effect of miRNAs on the protein levels of miRNA targets. *MIR3960* and *MIR4488* mimics at 50 nM significantly decreased the protein levels of CERS1 and NAT8L. Moreover, the *MIR3960* and *MIR4488* inhibitor increased the protein levels (**Fig. 5A-B**). Therefore, *MIR3960* and *MIR4488* modulate the levels of CERS1 and NAT8L.

A previous study shows that ATG13 is a target of *MIR4459*; however, an miRNA may have several targets,[28] so we studied other predicted targets of *MIR4459*. Among the predicted targets, we chose the one with the highest context score, LARP1. We transfected *MIR4459* mimics into both HEK293 cells and HUVECs, and found that LARP1 protein level was inhibited.(**Fig. 5C**)

Next, we cloned the 3′UTRs of *CERS1, NAT8L* and *LARP1* within the predicted binding sites of miRNAs into the luciferase reporter vector (**Fig. S2C**) and transfected the vectors into HEK293 cells with the corresponding miRNA mimics or the negative control. The luciferase activity was significantly decreased by the miRNAs as compared with the control (**Fig. 5D**). So *CERS1, NAT8L* and *LARP1* were directly targeted by *MIR3960, MIR4488* and *MIR4459*, respectively.

3BDO and TGFB2-OT1 overexpression regulated the protein levels of CERS1, NAT8L and LARP1

We further detected the role of *TGFB2-OT1* in the miRNA-targeted proteins. 3BDO treatment in HUVECs decreased the mRNA levels of *CERS1, LARP1* and *NAT8L* (**Fig. S4**), which was verified by western blot analysis of protein levels. Similarly, *TGFB2-OT1* downregulation by 3BDO dose-dependently decreased the protein levels of CERS1, NAT8L and LARP1 (**Fig. 6A-B**). Next, HEK293 cells were transfected with different amounts of pCMV6-*TGFB2-OT1* plasmid or pCMV6 plasmid as a control. *TGFB2-OT1* overexpression increased the protein levels of CERS1, NAT8L and LARP1.(**Fig. 6C-D**)

Overexpression of TGFB2-OT1 promoted translation of autophagy-related proteins

LARP1 is an RNA binding protein related to transcript stability and translation of mRNAs.[29] siRNA knocks down *LARP1* expression and inhibits global protein synthesis rates.[30] So we further investigated whether protein synthesis was affected by *TGFB2-OT1* and *MIR4459*. We first examined several proteins related to autophagy.

TGFB2-OT1 overexpression increased the protein levels of ATG3 and ATG7 (**Fig. S5**). SQSTM1 is the substrate of autophagic degradation.[31] However, SQSTM1 protein levels were greatly increased after HUVECs transfection with 0.01, 0.05,

0.1, 0.2 μg/ml pCMV6-*TGFB2-OT1* vector (**Fig. 7A**), and SQSTM1 puncta were increased in number in HUVECs treated with pCMV6-*TGFB2-OT1* plasmid (**Fig. 7B**). Furthermore, the mRNA level of *SQSTM1* was not increased in cells transfected with 0.1, 0.2 and 0.4 μg/ml pCMV6-*TGFB2-OT1* vector as compared with control transfection (**Fig. S6A**). In addition, 3BDO inhibited the increased SQSTM1 protein level induced by *TGFB2-OT1* (**Fig. S6B**) but did not affect the *SQSTM1* mRNA level (**Fig. S6C**).

We next investigated whether *TGFB2-OT1* regulated SQSTM1 expression via protein synthesis. *TGFB2-OT1* overexpression did not increase the level of SQSTM1 in the presence of cycloheximide, a well-known protein synthesis inhibitor (**Fig. 7C**). In addition, transfection with *MIR4459* mimics decreased SQSTM1 protein level, indicating that LARP1 was involved in SQSTM1 protein synthesis.(**Fig. 7D**)

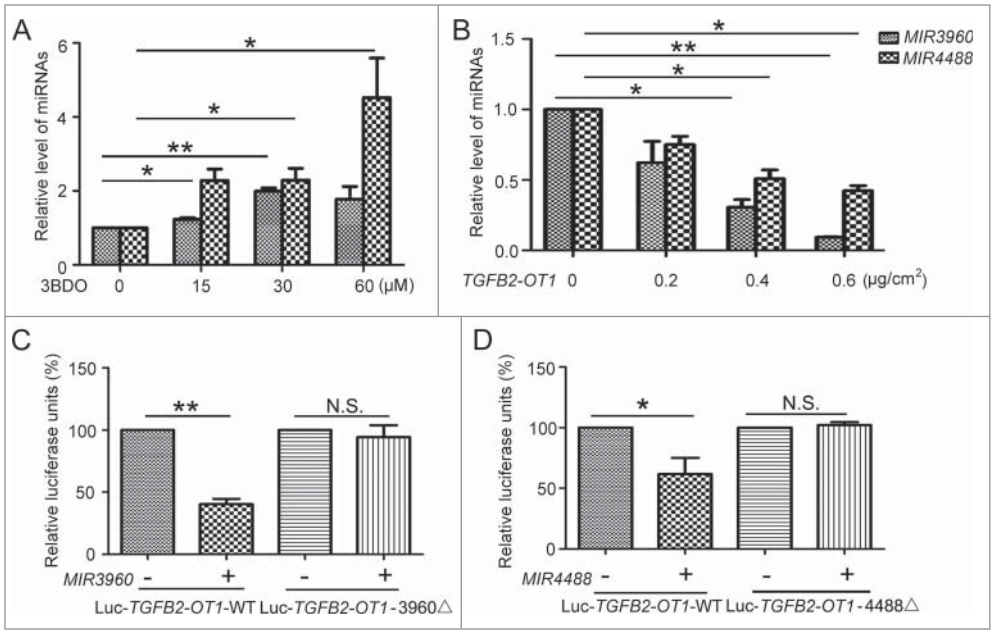

Figure 4. *MIR3960* and *MIR4488* directly bind to *TGFB2-OT1*. (**A**) qPCR analysis of *MIR3960* and *MIR4488* level in HUVECs treated with or without 3BDO (0, 15, 30 and 60 μM) for 24 h and (**B**) transfected with the empty vector pCMV6 (0.8 μg/cm^2, indicated by 0 in the figure) or pCMV6-*TGFB2-OT1* plasmid (0.2, 0.4 and 0.8 μg/cm^2) for 24 h. (**C**) Luciferase activity assay with Luc-*TGFB2-OT1*-WT and Luc-*TGFB2-OT1*-3960Δ plasmids cotransfected into HEK293 cells with 80 nM *MIR3960* mimics or negative control for 24 h. (**D**) Luciferase activity assay with Luc-*TGFB2-OT1*-WT and Luc-*TGFB2-OT1*-4488Δ plasmids cotransfected into HEK293 cells with 80 nM *MIR4488* mimics or negative control for 24 h. *, $P < 0.05$; **, $P < 0.01$; n = 3.

TGFB2-OT1 was involved in regulating NFKB RELA nuclear translocation and CASP1 activation in HUVECs

SQSTM1 is a receptor protein involved in both autophagy and inflammation. Therefore we deduced that *TGFB2-OT1* and *MIR4459* might participate in inflammation via SQSTM1. We first detected the location of the NFKB RELA by immunofluorescence assay. Overexpression of *TGFB2-OT1* significantly promoted NFKB RELA nuclear translocation (**Fig. 7E**, **Fig. S7A**). Furthermore, with *SQSTM1* knockdown, *TGFB2-OT1* overexpression did not induce RELA nuclear translocation. (**Fig. 7F**, **S7B and S7C**)

RELA plays a crucial role in inflammatory and immune responses. We found that overexpression of *TGFB2-OT1* in HUVECs promoted the production of IL6 and IL8 (**Fig. 7G**). Furthermore, *TGFB2-OT1* overexpression activated CASP1 and increased the *IL1B* mRNA level, which was inhibited by 3BDO (**Fig. 7H-I**). However, overexpression of *TGFB2-OT1* did not affect cell viability (**Fig. S7D**) or reactive oxygen species levels in HUVECs (**Fig. S7E**).

LOC100129973 (Genbank accession no. NR_102751.1, also known as AF007131) is annotated as an lncRNA in the NCBI database, but its functions have not been identified. We chose the lncRNA *LOC100129973* as the nonrelated lncRNA expression plasmid control to avoid a nonspecific, stress-related effect on the expression of the lncRNA. Transfection with pcDNA-*LOC100129973* plasmid did not affect SQSTM1 protein level or NFKB RELA nuclear translocation.(**Fig. S8**)

Discussion

Recent research has demonstrated that lncRNAs play an essential role in a number of cellular, developmental and pathological processes, such as cell apoptosis and differentiation,[32,33] tumorigenesis.[34] and X-inactivation.[35] Numerous reports suggest the existence of a widespread interaction network involving ceRNAs, with lncRNAs regulating miRNA by binding and titrating them off their binding sites on protein coding messengers. A recent study indicates that the lncRNA *MIAT* functions as a ceRNA and forms a feedback loop with vascular endothelial growth factor and *MIR150-5p* to regulate endothelial cell function.[36] However, the involvement of lncRNAs in endothelial cells biology is just beginning to be studied, and research of lncRNAs in controlling NFKB signaling and inflammation has mainly concentrated on other cell types such as macrophages.[37] Here, we verified that an lncRNA, *TGFB2-OT1* regulated autophagy and inflammation in VECs.

TGFB2-OT1 is a newly discovered lncRNA located in the 3′UTR of *TGFB2* and involved in VECs autophagy. In this study, we found that 2 inflammation inducers (LPS and oxLDL) promoted *TGFB2-OT1* expression, and the small chemical molecule 3BDO inhibited the increased *TGFB2-OT1* level in

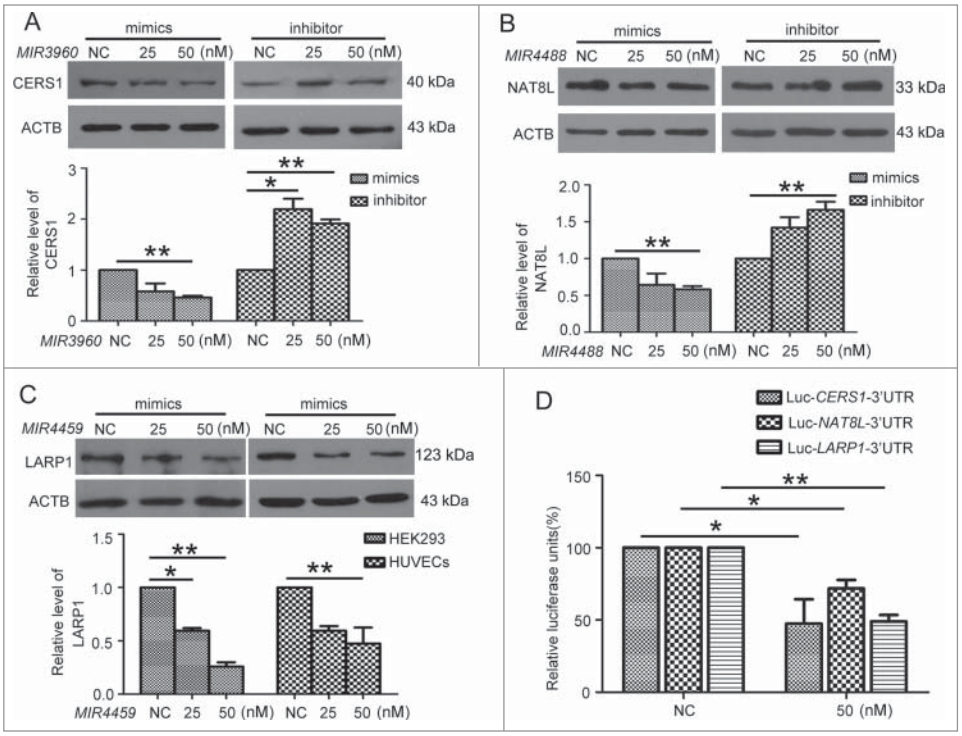

Figure 5. *MIR3960, MIR4488* and *MIR4459* targeted *CERS1, NAT8L* and *LARP1*. Western blot analysis of protein levels of CERS1 (**A**) and NAT8L (**B**) in HUVECs transfected with 25 and 50 nM *MIR3960* (**A**), *MIR4488* (**B**) mimics, inhibitor or negative control for 24 h and quantification. (**C**) Western blot analysis of protein levels of LARP1 in HEK293 cells (left) and HUVECs (right) transfected with 25 and 50 nM *MIR4459* mimics or negative control for 24 h and quantification. (**D**) Luciferase activity assay with Lu-*CERS1*-3′UTR, Lu-*NAT8L*-3′UTR, and Lu-*LARP1*-3′UTR plasmids cotransfected into HEK293 cells with 50 nM *MIR3960, MIR4488* and *MIR4459* mimics for 24 h, a negative miRNA as a control. *, $P < 0.05$; **, $P < 0.01$; n = 3.

HUVECs (**Fig. 1**). How LPS and oxLDL affect *TGFB2-OT1* production was not clear. Our previous study shows that LPS can increase NUPR1 protein level and autophagy in VECs, and 3BDO inhibits this effect.[25] We also discovered that TIA1 is responsible for *TGFB2-OT1* processing, and TIA1 phosphorylation inhibits *TGFB2-OT1* production.[19] In this study, we find that NUPR1 regulates *TGFB2-OT1* expression and acts upstream TIA1 (**Figs. 2 and 3**). LPS and oxLDL modulated *TGFB2-OT1* via NUPR1 and TIA1. Moreover, the TIA1 protein level was increased with siRNA-mediated knockdown of *NUPR1* (**Fig. 3D**, lane 3). NUPR1 is a stress-inducible nuclear protein involved in cellular stress responses as a transcription regulator. *NUPR1* deficiency induces apoptosis and intracellular reactive oxygen species level.[38-40] TIA1 is a proapoptosis protein involved in stress granule formation during cellular stress.[41-43] So the increase in TIA1 level might be due to the apoptosis and stress induced by *NUPR1* knockdown.

TGFB2-OT1 acts as a ceRNA, competes to bind with *MIR4459* and regulates the level of ATG13.[19] We have further determined the mechanisms by which *TGFB2-OT1* induced autophagy and inflammation. Here, we further identify 2 other miRNAs (*MIR3960* and *MIR4488*) that bind *TGFB2-OT1*.(**Fig. 4**)

A previous study indicates that mouse *Mir3960* promotes osteoblast differentiation by targeting HOXA2 (homeobox A2).[44] There are no reports about human *MIR3960* functions. Among the various predicted targets of *MIR3960*, we first selected CERS1. Luciferase activity assay confirmed the binding of *MIR3960* to the 3′UTR of *CERS1* (**Fig. 5D**). Ceramide synthases regulate the de novo generation of ceramides with specific fatty acid chain lengths.[45] CERS1 preferentially generates C18-ceramide. CERS1-driven production of C18-ceramide is defined as a tumor suppressor in preclinical and clinical research.[46] C18-ceramide induces autophagy via selective targeting of mitochondria by MAP1LC3B-containing phagophores via direct interaction between ceramide and MAP1LC3B on mitochondrial membranes.[47] Furthermore, excessive mitophagy induced by CERS1 is lethal and leads to tumor suppression.[26,47] *TGFB2-OT1* downregulation by 3BDO increased *MIR3960* levels and reduced those of CERS1, whereas *TGFB2-OT1* overexpression downregulated *MIR3960* levels and increased the CERS1 protein level (**Fig. 6**). CERS1 indirectly regulated by *TGFB2-OT1* contributes to explaining the autophagy alterations observed with changes in *TGFB2-OT1* level. Excessive promotion of CERS1 might lead to injury of VECs, which is consistent with overexpression of *TGFB2-OT1* inducing VECs inflammation.

So far, there are no studies of *MIR4488* functions. By using bioinformatics prediction analysis and luciferase activity assay (**Fig. 5D**), we found that NAT8L was an important target of *MIR4488*. NAT8L catalyzes the formation of N-acetylaspartate (NAA) from acetyl-CoA and aspartate. In the brain, NAA delivers the acetate moiety for synthesis of acetyl-CoA, which is further used for fatty acid generation.[48,49] Recent studies discovered new functions for NAT8L in adipose tissues. NAT8L is highly expressed in adipose tissues, murine and human adipogenic cell lines and localized in mitochondria of brown adipocytes. Upon NAT8L overexpression, mitochondrial mass and number as well as oxygen consumption are elevated.[27] So NAT8L may also be involved in autophagy by affecting mitochondria. *TGFB2-OT1* modulates NAT8L and then autophagy by sponging *MIR4488*.

LARP1 is an RNA binding protein and related to transcript stability and translation of mRNAs.[29,50] siRNA-depleted LARP1 level inhibits global protein synthesis rate.[30] As a ceRNA, *TGFB2-OT1* competed with *MIR4459* to modulate LARP1 protein level (**Fig. 6**). Previous studies show that *TGFB2-OT1* acts

downstream MTOR,[19] a master controller of protein synthesis, both in the initiation and elongation steps of protein synthesis.[14]

Here, we show that *TGFB2-OT1* overexpression increases ATG3, ATG7, and SQSTM1 protein levels (**Fig. 7A**, **Fig. S4**), which suggests that *TGFB2-OT1* is a key regulator in modulating protein synthesis. Furthermore, the decreased LARP1 protein level induced by *MIR4459* mimics transfection also decreased SQSTM1 expression (**Fig. 7D**), so *TGFB2-OT1* modulated SQSTM1 protein level by LARP1.

SQSTM1 acts as a signaling hub by recruiting and oligomerizing important signaling molecules in cytosolic speckles to determine cell survival or death by triggering the TRAF6-NFKB pathway or activating the aggregation of caspase 8 and its downstream effector caspases.[23,31] SQSTM1 similarly plays a role in the activation of CASP1, thereby inducing IL1B production, as an important component in the inflammasome complex.[24] The data showing that pCMV6-*TGFB2-OT1* elevated SQSTM1 but did not affect cell viability (Fig. S6C) indicate that caspase 8 and its downstream effector caspases were not activated. So we further examined the inflammation-related signal pathways.

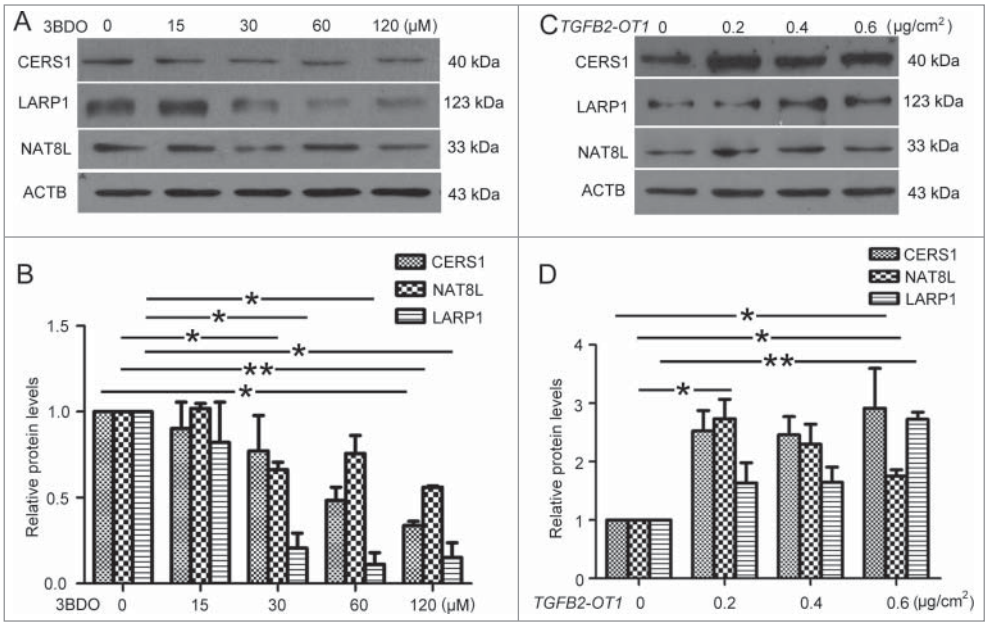

Figure 6. 3BDO and *TGFB2-OT1* overexpression regulated the protein levels of CERS1, LARP1 and NAT8L. (**A**) Western blot analysis of protein levels of CERS1, LARP1 and NAT8L in HUVECs treated with 3BDO (0, 15, 30, 60 and 120 μM) for 24 h and (**B**) quantification. (**C**) Western blot analysis of protein levels of CERS1, LARP1 and NAT8L in HEK293 cells transfected with the empty vector pCMV6 (0.8 μg/cm^2, indicated by 0 in the figure) or pCMV6-*TGFB2-OT1* plasmid (0.2, 0.4 and 0.8 μg/cm^2) for 48 h and (**D**) quantification. *, $P < 0.05$; **, $P < 0.01$; n = 3.

The evidence that overexpression of *TGFB2-OT1* induced NFKB RELA nuclear translocation and IL6 and IL8 production in VECs suggested that the NFKB pathway was activated (**Fig. 7E and G**). Furthermore, with *SQSTM1* knockdown, *TGFB2-OT1* overexpression did not induce RELA nuclear translocation (**Fig. 7F**). Activation of the NFKB pathway leads to the expression of various inflammation-associated genes, including cytokines, chemokines, and adhesion molecules.[51] Furthermore, *TGFB2-OT1* overexpression induced CASP1 activation and then *IL1B* expression (**Fig. 7H-I**), so *TGFB2-OT1* might be involved in activation of inflammasomes. Therefore, we demonstrated that *TGFB2-OT1* promoted inflammation responses via elevating SQSTM1 level. In contrast, a recent study shows that SQSTM1 deficiency in the tumor stroma results in the creation of a protumorigenic inflammatory environment driven by IL6.[52] SQSTM1 may present different outcomes depending on the cell type.

In summary, as shown in **Figure. 8**, lncRNA *TGFB2-OT1*, with decoy activity for *MIR3960, MIR4488* and *MIR4459* and by sequestering these miRNAs, increases the levels of CERS1, NAT8L, ATG13 and LARP1. LARP1 further elevates the levels of ATG3, ATG7 and SQSTM1, and then *TGFB2-OT1* promotes autophagy via CERS1, NAT8L, ATG13, ATG3 and ATG7 and participates in inflammation by promoting SQSTM1 protein synthesis and activating RELA and CASP1. LPS and oxLDL promotes *TGFB2-OT1* processing via NUPR1 and TIA1, so *TGFB2-OT1* is involved in autophagy and inflammation. 3BDO induces TIA1 phosphorylation via FKBP1A and MTORC1, which inhibits *TGFB2-OT1* processing,[19] then autophagy and inflammation as induced by *TGFB2-OT1*. Therefore, *TGFB2-OT1* is an attractive target against inflammation in VECs, and 3BDO might be a potential therapeutic compound for the development of new drugs for vascular diseases.

Materials and Methods

Cell culture and treatment

All cells were cultured at 37°C with 5% CO_2 in a humidified incubator. HUVECs were obtained as previously described,[53] and cultured in M199 medium (Gibco, 31100-035) with 10% fetal bovine serum (Hyclone, SV30087.02) and FGF2 (2 ng/ml). The cells used were not greater than passage 10. Human embryonic kidney 293 (HEK293) cells were cultured in DMEM medium (Gibco, 12800-017) with 10% fetal bovine serum. Cells at 80% confluence were activated by LPS (Sigma–Aldrich, L2880) and oxLDL (Biomedical Technologies Inc., BT-910). 3BDO was synthesized as described.[54] and dissolved in DMSO (0.1 M, Sigma-Aldrich, D2650) as a stock solution. DMSO

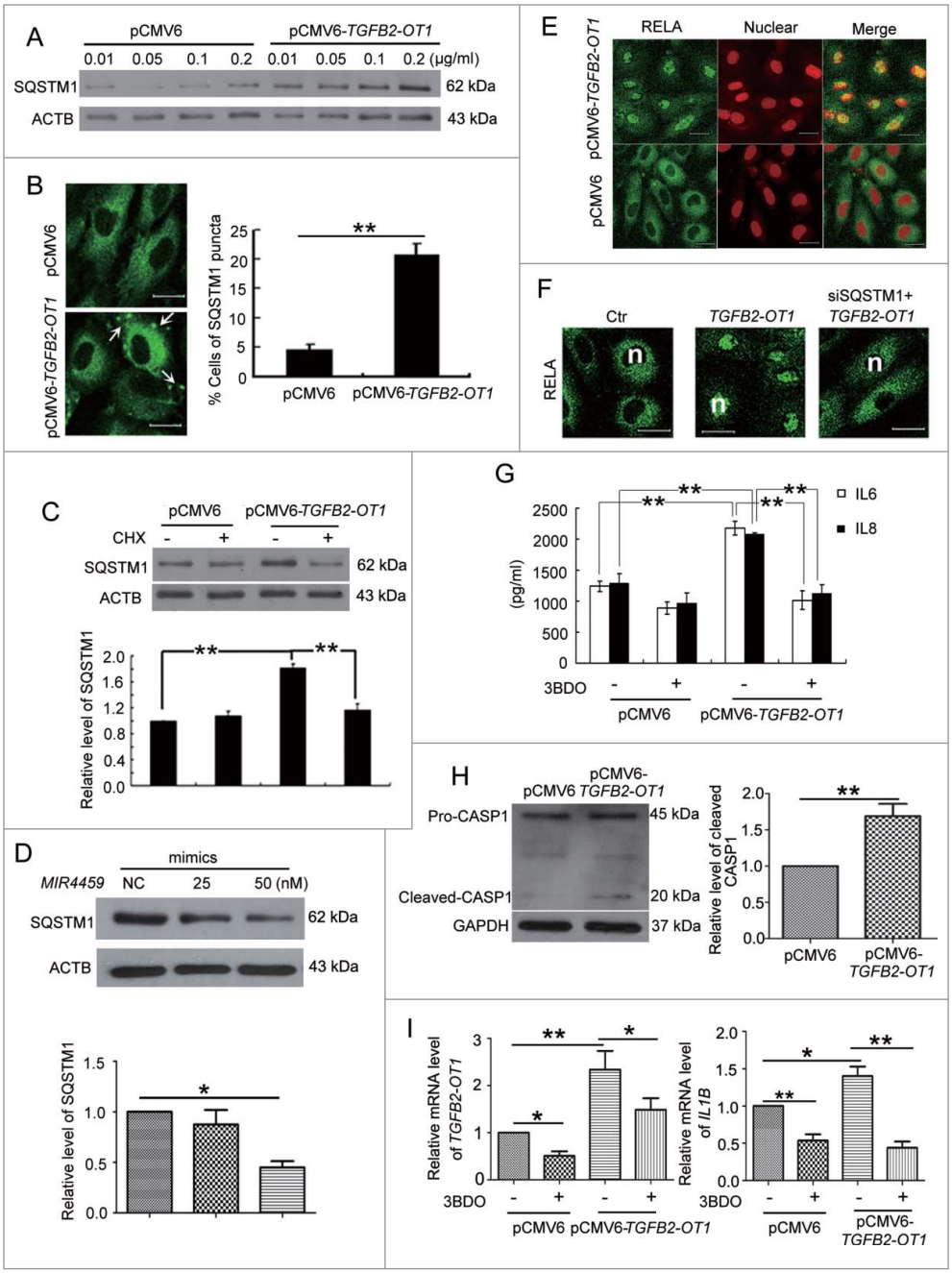

Figure 7. *TGFB2-OT1* promoted SQSTM1 translation, RELA nuclear translocation and IL6 and IL8 production in HUVECs. (**A**) Western blot analysis of SQSTM1 protein level in HUVECs transfected with 0.01, 0.05, 0.1, 0.2 μg/ml of pCMV6 or pCMV6-*TGFB2-OT1* for 48 h. This result is representative of 3 independent experiments. (**B**) Immunostaining of SQSTM1 in HUVECs transfected with pCMV6 or pCMV6-*TGFB2-OT1* (0.2 μg/ml) for 48 h, and the proportion of cells containing SQSTM1 puncta (> 5). The arrows indicate SQSTM1 puncta in cells. Bar: 16 μm. (**C**) Western blot analysis of SQSTM1 protein level in HUVECs transfected with pCMV6 or pCMV6-*TGFB2-OT1* (0.2 μg/ml) for 12 h, then treated with or without cycloheximide (CHX) for 12 h. (**D**) Western blot analysis of SQSTM1 protein level in HUVECs transfected with 25 and 50 nM *MIR4459* mimics or negative control for 24 h. (**E**) Representative photomicrographs of immunofluorescence staining showing RELA nuclear translocation in HUVECs transfected with pCMV6 or pCMV6-*TGFB2-OT1* (0.4 μg/ml) for 48 h. Bar: 16 μm. (**F**) Immunofluorescent graphs of RELA nuclear translocation in HUVECs transfected with pCMV6, pCMV6-*TGFB2-OT1*, or both siRNA against *SQSTM1* and pCMV6-*TGFB2-OT1* for 48 h. n indicates the nuclear. Bar: 16 μm. (**G**) ELISA of IL6 and IL8 production in HUVECs transfected with 0.4 μg/ml pCMV6 or pCMV6-*TGFB2-OT1* for 48 h, then exposed to 3BDO (60 μM) for 6 h. (**H**) Western blot analysis of cleaved-CASP1 protein level in HUVECs transfected with 0.4 μg/ml pCMV6 or pCMV6-*TGFB2-OT1* for 48 h and quantification. (**I**) qPCR analysis of mRNA levels of *TGFB2-OT1* and *IL1B* in HUVECs transfected with 0.4 μg/ml pCMV6 or pCMV6-*TGFB2-OT1* for 48 h, then exposed to 3BDO (60 μM) for 12 h. *, $P < 0.05$; **, $P < 0.01$; n = 3.

used in the experiment was below 0.1% in culture medium (v/v) and did not affect cell viability.

RNA interference

The efficiency of TIA1.[19] and NUPR1.[25] silencing was previously described. Cells at 50% to 60% confluence were transfected with *TIA1* (Santa Cruz Biotechnology, sc-29504), *NUPR1* (Santa Cruz Biotechnology, sc-40792) or scrambled siRNA (Santa Cruz Biotechnology, sc-37007) for 24 h by use of RNAiFect Transfection Reagent according to the manufacturer's protocol (QIAGEN, 301605). The efficiency of RNA interference was determined by protein gel blot analysis.

Plasmid transfection

Cells were seeded onto 6-cm dishes at 1×10^6/mL and grown for 24 h. Cells at 70% to 80% confluence were transfected with the indicated expression vectors by use of Lipofectamine 2000 transfection reagent (Invitrogen, 11668019) according to the manufacturer's protocol. The pCMV6-*TGFB2-OT1* vector was generated as previously reported.[19]

Luciferase activity assay

A luciferase reporter vector (pmirGLO Dual-Luciferase miRNA Target Expression Vector; Promega) was used for the luciferase constructs. The *TGFB2-OT1*, 3′UTRs of *CERS1, NAT8L* and *LARP1* were cloned by RT-PCR, then Luc-*TGFB2-OT1*-WT, mutants, Luc-*CERS1*-3′UTR, Luc-*NAT8L*-3′UTR and Luc-*LARP1*-3′UTR were constructed as previously reported.[19] HEK293 cells were seeded onto 96-well culture plates at 8000 cells per well in DMEM medium containing 10% fetal bovine serum and incubated overnight. Cells were cotransfected with Dual-Luciferase (containing Firefly and Renilla luciferase) reporter

constructs and corresponding miRNA mimics or negative control by Lipofectamine 2000 transfection reagent (Invitrogen, 11668019). After transfection for 24 h, luciferase activity assays were determined by a dual-luciferase reporter system according to the protocol (Promega, E2920).

RT-PCR and quantitative real-time PCR (qPCR)

Total RNA was extracted from cells with use of TriZol Reagent (Sigma-Aldrich, T9424) following the manufacturer's protocol. An amount of 1 μg RNA was reverse-transcribed by use of the PrimeScript RT reagent Kit with gDNA Eraser (TaKaRa, DRR047A). qPCR reactions involved use of the QuantiTect SYBR Green PCR kit (Takara, RR420) and LightCycler 2.0 system (Roche, Basel, Switzerland). Reactions were carried out in a 20 μl volume containing 10 μl 2×SYBR Green PCR Master Mix. The primer pair sequences were for *TGFB2-OT1*, forward 5'-GCAGTTTCACCTAAAGAGCAGC-3′, and reverse 5'-TTCCTTCCCACCTCCACCC-3′; and GAPDH, forward, 5′-ACCACAGTCCATGCCAT-CAC-3′, and reverse, 5′-TCCAC-CACCCTGTTGCTGTA-3′ as a housekeeping gene. The rest of primer sequences are listed in **Table S1**. The fold changes in mRNA level were calculated by use of MxPro v4.00 (Stratagene). Relative gene expression was normalized to the *GAPDH* level.

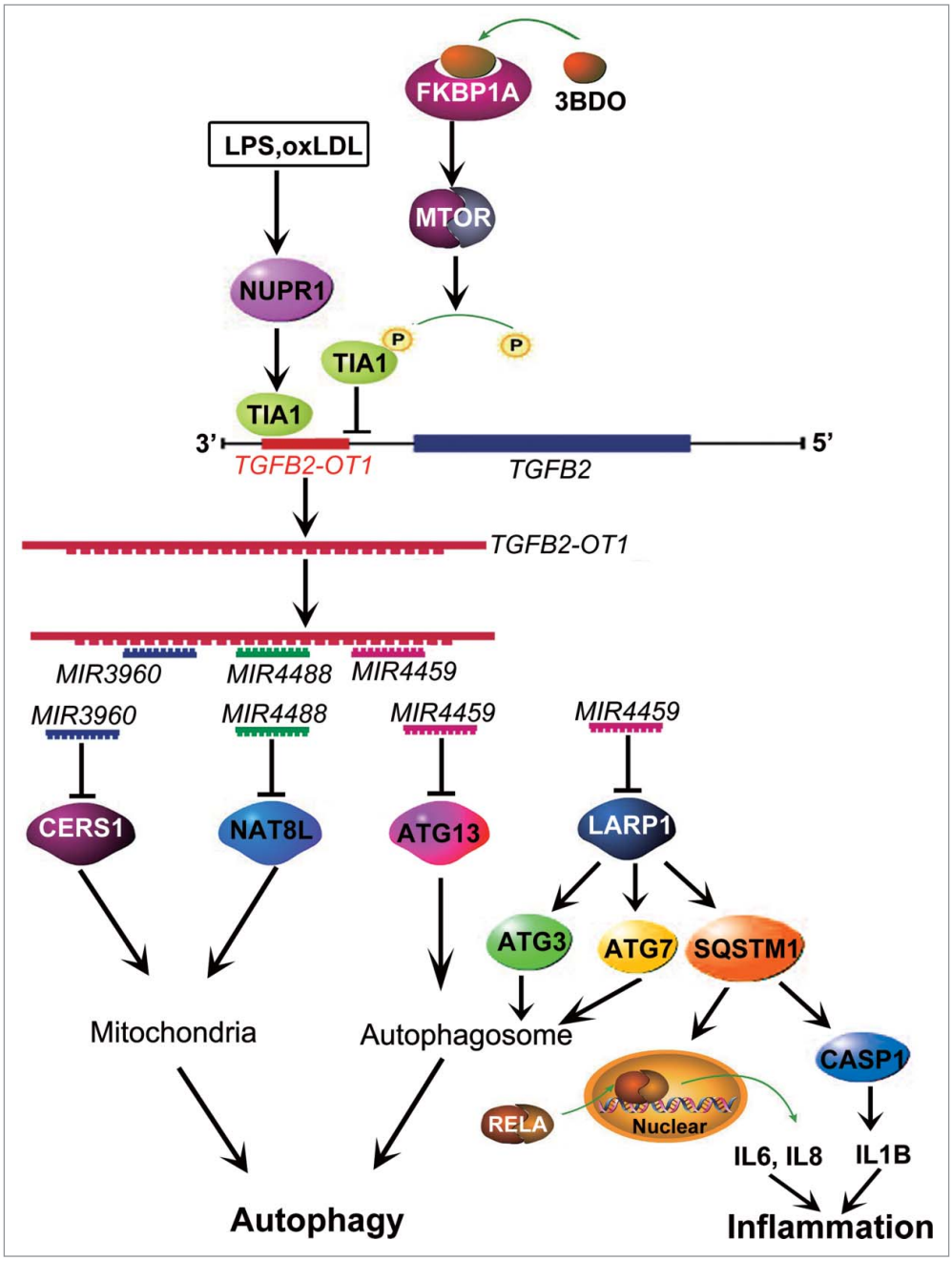

Figure 8. Conceptual schematic of the miRNA signal pathway regulated by *TGFB2-OT1* in autophagy and inflammation. LPS and oxLDL promote TIA1 expression via NUPR1. TIA1 is responsible for *TGFB2-OT1* processing from 3′UTR of *TGFB2*. *TGFB2-OT1*, as a miRNA sponge, decoys *MIR3960, MIR4488*, and *MIR4459*, then elevates CERS1, NAT8L, ATG13, and LARP1 protein levels. LARP1 further increases the levels of ATG3, ATG7 and SQSTM1. CERS1 and NAT8L regulate autophagy by affecting mitochondria. ATG13, ATG3 and ATG7 modulate autophagy. The elevated synthesis of SQSTM1 protein activates RELA and CASP1, increase levels of inflammatory cytokines IL6, IL8 and IL1B, and thereby induce inflammation. 3BDO induces TIA1 phosphorylation via FKBP1A and MTORC1, which may result in inhibition of *TGFB2-OT1* processing, autophagy and inflammation induced by *TGFB2-OT1*.

Western blot analysis

Cell lysates were prepared in RIPA lysis buffer (Beyotime, P0013B) containing 1 mM PMSF. Equal amounts of proteins were run on SDS-polyacrylamide gel, then transferred to polyvinylidene difluoride (PVDF) membrane (Millipore, IPFL00010), probed with primary antibodies, horseradish peroxidase-linked secondary antibodies (Santa Cruz Biotechnology, sc-2004 and sc-2302), and detected with use of an enhanced chemiluminesence detection kit (Thermo, 32209). The primary antibodies specific to GAPDH (sc-47724), TIA1 (sc-166247),

CERS1 (sc-135033), LARP1 (sc-102006), and RELA (sc-372) were from Santa Cruz Biotechnology. Antibody for SQSTM1 (610833) was from BD Transduction Laboratories. Antibodies for ACTB (A5441), NUPR1 (SAB1104559) and NAT8L (HPA040677) were from Sigma-Aldrich. Antibodies for ATG3 (3415), ATG7 (8558) and CASP1 (2225) were from Cell Signaling Technology. The relative quantity of proteins was analyzed by ImageJ software and normalized to loading controls.

In situ hybridization

In situ hybridization to detect *TGFB2-OT1* expression in HUVECs was performed as described by Roche Applied Science. Briefly, cells were fixed in 4% paraformaldehyde. Then the cells were rehydrated, digested and then refixed in 4% paraformaldehyde. After that, the cells were prehybridized with hybridization solution and then incubated with a digoxigenin-labeled *TGFB2-OT1* probe at 42°C for 20 h. The next day, the cells were washed with 2× SSC, 1× SSC and 0.5× SSC and then incubated with a mouse anti-digoxin antibody conjugated with alkaline phosphatase (Sigma-Aldrich, A1054). For visualizing the positive signal, the sections were incubated in NBT/BCIP (Roche, 11681451001) and counterstained with nuclear fast red (Sigma-Aldrich, N8002). Staining of treated samples was performed for an equal length of time and experiments were repeated at least 3 times.

Immunofluorescence assay of cells

Immunofluorescence assay was performed as described.[19] In brief, after treatment, HUVECs were fixed with 4% paraformaldehyde for 15 min and blocked with 3% normal goat serum (ZSGB-BIO, ZLI-9026) or rabbit serum (ZSGB-BIO, ZLI-9026) for 20 min at room temperature. Then, the cells were incubated with primary antibody (1:100) at 4°C overnight and then corresponding secondary antibody (1:200) at 37°C for 1 h. Cells were rinsed 3 times with 0.1 M phosphate-buffered saline (PBS; 137 mM NaCl, 2.7 mM KCl, 10 mM Na2HPO4, 2 mM KH2PO4) to eliminate the uncombined secondary antibody. The samples were evaluated by Zeiss LSM700 (Carl Zeiss, Oberkochen, Germany).

Quantitative real-time PCR of miRNA expression

RNA was isolated with the Trizol reagent method. RNA samples were quantified by use of the NanoDrop. MiRNA was converted into cDNA by using TaqMan MicroRNA Reverse Transcription Kit (Applied Biosystems, PN4366596) and specific miRNA primers. The KAPA SYBR FAST qPCR Kits (Kapa Biosystems, KK4601) was used to quantify the expression of mature miRNA in HUVECs. Quantitative real-time PCR reactions involved use of the LightCycler 480 Real-Time PCR System (Roche, Basel, Switzerland). Following a single cycle at 95°C for 10 min, PCR involved 40 cycles at 95°C for 30 sec and 60°C for 1 min. MiRNA expression was calculated as relative to *RNU6* expression, by independent triplicate measurements. The primer sequences used for *MIR3960* (stem-loop primer): 5′-GTCGTATCCAGTGCAGGGTCCGAGGTATTCGCA CTGGATACGACCCCCGCC-3′, (PCR primer): 5′-ATT-TAAGGCGGCGGCGGA-3′; *MIR4488* (stem-loop primer): 5′-GTCGTATCCAGTGCAGGGTCCGAGG-TATTCGCA CTGGATACGACGCCGGAG-3′, (PCR primer) 5′-TAATAAAGGGGGCGGGCT-3′; and *RNU6*, 5′-CTCGCTTCGGCAGCACATATACT-3′, 5′-ACGCTT-CACGAATTTGCGTGTC-3′.

Transfection with miRNA mimics and inhibitor

RNA mimics and inhibitor for *MIR3960, MIR4488, MIR4459* and negative control (NC) were designed and purchased from Invitrogen. The mimics and inhibitors were transfected into HUVECs or HEK293 cells with RNAiFect Transfection Reagent according to the manufacturer's protocol for 24 h. The final concentrations of the mimics or inhibitors were 25 or 50 nM.

Statistical analysis

All experiments were repeated independently for at least 3 times. Data are expressed as mean ± SE. SPSS 11.5 (SPSS Inc., Chicago, IL) was used for analysis by one-way ANOVA (followed by Scheffé F test for post-hoc analysis). A $P < 0.05$ was considered as statistically significant.

Disclosure of Potential Conflicts of Interest

No potential conflicts of interest were disclosed.

Funding

This work was supported by the National Natural Science Foundation of China (No. 91313303, 81321061, 91539105, 31270877, 20972088, 31070735, and 31501122) and the National 973 Research Project (No. 2011CB503906).

Supplemental Material

Supplemental data for this article can be accessed on the publisher's website.

References

1. Ronnau CG, Verhaegh GW, Luna-Velez MV, Schalken JA. Noncoding RNAs as novel biomarkers in prostate cancer. Biomed Res Internatl 2014; 2014:591703; http://dx.doi.org/10.1155/2014/591703
2. Perkel JM. Visiting "noncodarnia." Biotechniques 2013; 54:301, 3-4
3. Clark MB, Amaral PP, Schlesinger FJ, Dinger ME, Taft RJ, Rinn JL, Ponting CP, Stadler PF, Morris KV, Morillon A, et al. The reality of pervasive transcription. PLoS Biol 2011; 9:e1000625; discussion e1102; http://dx.doi.org/10.1371/journal.pbio.1000625
4. van Bakel H, Nislow C, Blencowe BJ, Hughes TR. Most "dark matter" transcripts are associated with known genes. PLoS Biol 2010; 8:e1000371; PMID:20502517; http://dx.doi.org/10.1371/journal.pbio.1000371
5. Heard E, Disteche CM. Dosage compensation in mammals: fine-tuning the expression of the X chromosome. Genes Dev 2006; 20:1848-67; PMID:16847345; http://dx.doi.org/10.1101/gad.1422906
6. Payer B, Lee JT. X chromosome dosage compensation: how mammals keep the balance. Ann Rev Genet 2008; 42:733-72; PMID:18729722; http://dx.doi.org/10.1146/annurev.genet.42.110807.091711
7. Hung T, Chang HY. Long noncoding RNA in genome regulation: prospects and mechanisms. RNA Biol 2010; 7:582-5; PMID:20930520; http://dx.doi.org/10.4161/rna.7.5.13216
8. Rapicavoli NA, Poth EM, Blackshaw S. The long noncoding RNA RNCR2 directs mouse retinal cell

specification. BMC Dev Biol 2010; 10:49; PMID:20459797; http://dx.doi.org/10.1186/1471-213X-10-49
9. Tripathi V, Ellis JD, Shen Z, Song DY, Pan Q, Watt AT, Freier SM, Bennett CF, Sharma A, Bubulya PA, et al. The nuclear-retained noncoding RNA MALAT1 regulates alternative splicing by modulating SR splicing factor phosphorylation. Mol Cell 2010; 39:925-38; PMID:20797886; http://dx.doi.org/10.1016/j.molcel.2010.08.011
10. Moreno-Moya JM, Vilella F, Simon C. MicroRNA: key gene expression regulators. Fertility Sterility 2014; 101:1516-23; PMID:24314918; http://dx.doi.org/10.1016/j.fertnstert.2013.10.042
11. Yoon JH, Abdelmohsen K, Gorospe M. Functional interactions among microRNAs and long noncoding RNAs. Seminars Cell Dev Biol 2014; 34:9-14; http://dx.doi.org/10.1016/j.semcdb.2014.05.015
12. Yoon JH, Abdelmohsen K, Srikantan S, Yang X, Martindale JL, De S, Huarte M, Zhan M, Becker KG, Gorospe M. LincRNA-p21 suppresses target mRNA translation. Mol Cell 2012; 47:648-55; PMID:22841487; http://dx.doi.org/10.1016/j.molcel.2012.06.027
13. Yoon JH, Abdelmohsen K, Kim J, Yang X, Martindale JL, Tominaga-Yamanaka K, White EJ, Orjalo AV, Rinn JL, Kreft SG, et al. Scaffold function of long noncoding RNA HOTAIR in protein ubiquitination. Nature Commun 2013; 4:2939; http://dx.doi.org/10.1038/ncomms3939
14. Faghihi MA, Zhang M, Huang J, Modarresi F, Van der Brug MP, Nalls MA, Cookson MR, St-Laurent G, 3rd, Wahlestedt C. Evidence for natural antisense transcript-mediated inhibition of microRNA function. Genome Biol 2010; 11:R56; PMID:20507594; http://dx.doi.org/10.1186/gb-2010-11-5-r56
15. Cesana M, Cacchiarelli D, Legnini I, Santini T, Sthandier O, Chinappi M, Tramontano A, Bozzoni I. A long noncoding RNA controls muscle differentiation by functioning as a competing endogenous RNA. Cell 2011; 147:358-69; PMID:22000014; http://dx.doi.org/10.1016/j.cell.2011.09.028
16. Keniry A, Oxley D, Monnier P, Kyba M, Dandolo L, Smits G, Reik W. The H19 lincRNA is a developmental reservoir of miR-675 that suppresses growth and Igf1r. Nat Cell Biol 2012; 14:659-65; PMID:22684254; http://dx.doi.org/10.1038/ncb2521
17. Salmena L, Poliseno L, Tay Y, Kats L, Pandolfi PP. A ceRNA hypothesis: the Rosetta Stone of a hidden RNA language? Cell 2011; 146:353-8; PMID:21802130; http://dx.doi.org/10.1016/j.cell.2011.07.014
18. Poliseno L, Salmena L, Zhang J, Carver B, Haveman WJ, Pandolfi PP. A coding-independent function of gene and pseudogene mRNAs regulates tumour biology. Nature 2010; 465:1033-8; PMID:20577206; http://dx.doi.org/10.1038/nature09144
19. Ge D, Han L, Huang S, Peng N, Wang P, Jiang Z, Zhao J, Su L, Zhang S, Zhang Y, et al. Identification of a novel MTOR activator and discovery of a competing endogenous RNA regulating autophagy in vascular endothelial cells. Autophagy 2014; 10:957-71; PMID:24879147; http://dx.doi.org/10.4161/auto.28363
20. Peng N, Meng N, Wang S, Zhao F, Zhao J, Su L, Zhang S, Zhang Y, Zhao B, Miao J. An activator of mTOR inhibits oxLDL-induced autophagy and apoptosis in vascular endothelial cells and restricts atherosclerosis in apolipoprotein E(-)/(-) mice. Scientific Rep 2014; 4:5519
21. Jones SA, Mills KH, Harris J. Autophagy and inflammatory diseases. Immunol Cell Biol 2013; 91:250-8; PMID:23318657; http://dx.doi.org/10.1038/icb.2012.82
22. Levine B, Mizushima N, Virgin HW. Autophagy in immunity and inflammation. Nature 2011; 469:323-35; PMID:21248839; http://dx.doi.org/10.1038/nature09782
23. Manley S, Williams JA, Ding WX. Role of p62/SQSTM1 in liver physiology and pathogenesis. Exp Biol Med 2013; 238:525-38; http://dx.doi.org/10.1177/1535370213489446
24. Choe JY, Jung HY, Park KY, Kim SK. Enhanced p62 expression through impaired proteasomal degradation is involved in caspase-1 activation in monosodium urate crystal-induced interleukin-1b expression. Rheumatology 2014; 53:1043-53; PMID:24587486; http://dx.doi.org/10.1093/rheumatology/ket474
25. Meng N, Zhao J, Su L, Zhao B, Zhang Y, Zhang S, Miao J. A butyrolactone derivative suppressed lipopolysaccharide-induced autophagic injury through inhibiting the autoregulatory loop of p8 and p53 in vascular endothelial cells. Int J Biochem Cell Biol 2012; 44:311-9; PMID:22085531; http://dx.doi.org/10.1016/j.biocel.2011.11.001
26. Jiang W, Ogretmen B. Ceramide stress in survival versus lethal autophagy paradox: ceramide targets autophagosomes to mitochondria and induces lethal mitophagy. Autophagy 2013; 9:258-9; PMID:23182807; http://dx.doi.org/10.4161/auto.22739
27. Pessentheiner AR, Pelzmann HJ, Walenta E, Schweiger M, Groschner LN, Graier WF, Kolb D, Uno K, Miyazaki T, Nitta A, et al. NAT8L (N-acetyltransferase 8-like) accelerates lipid turnover and increases energy expenditure in brown adipocytes. J Biol Chem 2013; 288:36040-51; PMID:24155240; http://dx.doi.org/10.1074/jbc.M113.491324
28. Krek A, Grun D, Poy MN, Wolf R, Rosenberg L, Epstein EJ, MacMenamin P, da Piedade I, Gunsalus KC, Stoffel M, et al. Combinatorial microRNA target predictions. Nat Genet 2005; 37:495-500; PMID:15806104; http://dx.doi.org/10.1038/ng1536
29. Blagden SP, Gatt MK, Archambault V, Lada K, Ichihara K, Lilley KS, Inoue YH, Glover DM. Drosophila Larp associates with poly(A)-binding protein and is required for male fertility and syncytial embryo development. Dev Biol 2009; 334:186-97; PMID:19631203; http://dx.doi.org/10.1016/j.ydbio.2009.07.016
30. Burrows C, Abd Latip N, Lam SJ, Carpenter L, Sawicka K, Tzolovsky G, Gabra H, Bushell M, Glover DM, Willis AE, et al. The RNA binding protein Larp1 regulates cell division, apoptosis and cell migration. Nucleic Acids Res 2010; 38:5542-53; PMID:20430826; http://dx.doi.org/10.1093/nar/gkq294
31. Pursiheimo JP, Rantanen K, Heikkinen PT, Johansen T, Jaakkola PM. Hypoxia-activated autophagy accelerates degradation of SQSTM1/p62. Oncogene 2009; 28:334-44; PMID:18931699; http://dx.doi.org/10.1038/onc.2008.392
32. Huarte M, Guttman M, Feldser D, Garber M, Koziol MJ, Kenzelmann-Broz D, Khalil AM, Zuk O, Amit I, Rabani M, et al. A large intergenic noncoding RNA induced by p53 mediates global gene repression in the p53 response. Cell 2010; 142:409-19; PMID:20673990; http://dx.doi.org/10.1016/j.cell.2010.06.040
33. Hu W, Alvarez-Dominguez JR, Lodish HF. Regulation of mammalian cell differentiation by long non-coding RNAs. EMBO Rep 2012; 13:971-83; PMID:23070366; http://dx.doi.org/10.1038/embor.2012.145
34. Gupta RA, Shah N, Wang KC, Kim J, Horlings HM, Wong DJ, Tsai MC, Hung T, Argani P, Rinn JL, et al. Long non-coding RNA HOTAIR reprograms chromatin state to promote cancer metastasis. Nature 2010; 464:1071-6; PMID:20393566; http://dx.doi.org/10.1038/nature08975
35. Lee JT, Bartolomei MS. X-inactivation, imprinting, and long noncoding RNAs in health and disease. Cell 2013; 152:1308-23; PMID:23498939; http://dx.doi.org/10.1016/j.cell.2013.02.016
36. Yan B, Liu J, Yao J, Li X, Wang X, Li Y, Tao Z, Song Y, Chen Q, Jiang Q. LncRNA-MIAT Regulates Microvascular Dysfunction by Functioning as a Competing Endogenous RNA. Circ Res 2015; 116(7):1143-56; PMID:25587098; http://dx.doi.org/10.1161/CIRCRESAHA.116.305510
37. Carpenter S, Aiello D, Atianand MK, Ricci EP, Gandhi P, Hall LL, Byron M, Monks B, Henry-Bezy M, Lawrence JB, et al. A long noncoding RNA mediates both activation and repression of immune response genes. Science 2013; 341:789-92; PMID:23907535; http://dx.doi.org/10.1126/science.1240925
38. Chen SS, Hu W, Wang Z, Lou XE, Zhou HJ. p8 attenuates the apoptosis induced by dihydroartemisinin in cancer cells through promoting autophagy. Cancer Biol Ther 2015; 16(5):1-10
39. Weis S, Schlaich TC, Dehghani F, Carvalho T, Sommerer I, Fricke S, Kahlenberg F, Mossner J, Hoffmeister A. p8 Deficiency causes siderosis in spleens and lymphocyte apoptosis in acute pancreatitis. Pancreas 2014; 43:1277-85; PMID:25098696; http://dx.doi.org/10.1097/MPA.0000000000000172
40. Weis S, Bielow T, Sommerer I, Iovanna J, Malicet C, Mossner J, Hoffmeister A. P8 deficiency increases cellular ROS and induces HO-1. Arch Biochem Biophy 2015; 565:89-94; http://dx.doi.org/10.1016/j.abb.2014.11.007
41. Sanchez-Jimenez C, Ludena MD, Izquierdo JM. T-cell intracellular antigens function as tumor suppressor genes. Cell Death Dis 2015; 6:e1669; PMID:25741594; http://dx.doi.org/10.1038/cddis.2015.43
42. Forch P, Valcarcel J. Molecular mechanisms of gene expression regulation by the apoptosis-promoting protein TIA-1. Apoptosis 2001; 6:463-8; http://dx.doi.org/10.1023/A:1012441824719
43. Anderson P, Kedersha N. Visibly stressed: the role of eIF2, TIA-1, and stress granules in protein translation. Cell Stress Chaperones 2002; 7:213-21; PMID:12380690; http://dx.doi.org/10.1379/1466-1268(2002)007<0213:VSTROE>2.0.CO;2
44. Hu R, Liu W, Li H, Yang L, Chen C, Xia ZY, Guo LJ, Xie H, Zhou HD, Wu XP, et al. A Runx2/miR-3960/miR-2861 regulatory feedback loop during mouse osteoblast differentiation. J Biol Chem 2011; 286:12328-39; PMID:21324897; http://dx.doi.org/10.1074/jbc.M110.176099
45. Pewzner-Jung Y, Ben-Dor S, Futerman AH. When do Lasses (longevity assurance genes) become CerS (ceramide synthases)?: Insights into the regulation of ceramide synthesis. J Biol Chem 2006; 281:25001-5; PMID:16793762; http://dx.doi.org/10.1074/jbc.R600010200
46. Saddoughi SA, Garrett-Mayer E, Chaudhary U, O'Brien PE, Afrin LB, Day TA, Gillespie MB, Sharma AK, Wilhoit CS, Bostick R, et al. Results of a phase II trial of gemcitabine plus doxorubicin in patients with recurrent head and neck cancers: serum C(1)(8)-ceramide as a novel biomarker for monitoring response. Clin Cancer Res 2011; 17:6097-105; PMID:21791630; http://dx.doi.org/10.1158/1078-0432.CCR-11-0930
47. Sentelle RD, Senkal CE, Jiang W, Ponnusamy S, Gencer S, Selvam SP, Ramshesh VK, Peterson YK, Lemasters JJ, Szulc ZM, et al. Ceramide targets autophagosomes to mitochondria and induces lethal mitophagy. Nat Chem Biol 2012; 8:831-8; PMID:22922758; http://dx.doi.org/10.1038/nchembio.1059
48. Wiame E, Tyteca D, Pierrot N, Collard F, Amyere M, Noel G, Desmedt J, Nassogne MC, Vikkula M, Octave JN, et al. Molecular identification of aspartate N-acetyltransferase and its mutation in hypoacetylaspartia. Biochem J 2010; 425:127-36; http://dx.doi.org/10.1042/BJ20091024
49. Ariyannur PS, Moffett JR, Manickam P, Pattabiraman N, Arun P, Nitta A, Nabeshima T, Madhavarao CN, Namboodiri AM. Methamphetamine-induced neuronal protein NAT8L is the NAA biosynthetic enzyme:

implications for specialized acetyl coenzyme A metabolism in the CNS. Brain Res 2010; 1335:1-13; PMID:20385109; http://dx.doi.org/10.1016/j.brainres.2010.04.008
50. Moscat J, Diaz-Meco MT. The atypical protein kinase Cs. Functional specificity mediated by specific protein adapters. EMBO Rep 2000; 1:399-403; PMID:11258478; http://dx.doi.org/10.1093/embo-reports/kvd098
51. Dryden NH, Sperone A, Martin-Almedina S, Hannah RL, Birdsey GM, Khan ST, Layhadi JA, Mason JC, Haskard DO, Gottgens B, et al. The transcription factor Erg controls endothelial cell quiescence by repressing activity of nuclear factor (NF)-kappaB p65. J biol Chem 2012; 287:12331-42; PMID:22337883; http://dx.doi.org/10.1074/jbc.M112.346791
52. Valencia T, Kim JY, Abu-Baker S, Moscat-Pardos J, Ahn CS, Reina-Campos M, Duran A, Castilla EA, Metallo CM, Diaz-Meco MT, et al. Metabolic Reprogramming of Stromal Fibroblasts through p62-mTORC1 Signaling Promotes Inflammation and Tumorigenesis. Cancer Cell 2014; 26:121-35; PMID:25002027; http://dx.doi.org/10.1016/j.ccr.2014.05.004
53. Jaffe EA, Nachman RL, Becker CG, Minick CR. Culture of human endothelial cells derived from umbilical veins. Identification by morphologic and immunologic criteria. J Clin Invest 1973; 52:2745-56; PMID:4355998; http://dx.doi.org/10.1172/JCI107470
54. Wang W, Liu X, Zhao J, Zhao B, Zhang S, Miao J. A novel butyrolactone derivative inhibited apoptosis and depressed integrin beta4 expression in vascular endothelial cells. Bioorganic Med Chem Lett 2007; 17:482-5; http://dx.doi.org/10.1016/j.bmcl.2006.10.023